

INTERNATIONAL SOCIETY FOR SOIL MECHANICS AND GEOTECHNICAL ENGINEERING



This paper was downloaded from the Online Library of the International Society for Soil Mechanics and Geotechnical Engineering (ISSMGE). The library is available here:

<https://www.issmge.org/publications/online-library>

This is an open-access database that archives thousands of papers published under the Auspices of the ISSMGE and maintained by the Innovation and Development Committee of ISSMGE.

Interaction between Soil and Grouted Anchor

Interaction entre Sol et Ancre Injectée

G. PETRASOVITS D. Sc., Civ. Eng., Professor of Geotechnical Engineering, Technical University of Budapest

SYNOPSIS

Based on the analysis of the behaviour of long time monitored instrumented anchors author arrived at the conclusion that the value of the shear resistance along the bond length in granular soils was influenced mainly by the initial or relative density of the soil, its grain size distribution and the grouting pressure. The treatise gives a calculation method to predict the carrying capacity and the displacement of anchors after presenting the test results and the load transfer mechanism. The applicability of the proposed calculation method is demonstrated on a practical example and the factors affecting the mobilized length of shear resistance is analyzed.

INTRODUCTION

Great attention is paid by the researchers to further develop the existing methods used for the load carrying capacity of grouted anchors or to elaborate new ones. The efforts made to achieve this aim can lead to results only if the behaviour under load of the grouted anchors widely used in civil engineering is analysed on a complex way, in other words, it includes the investigation of the numerous factors affecting the amount and distribution of shearing resistance along the bond length. This treatise intends to review the field tests and theoretical investigations carried out recently in connection with this problem complex. The civil engineering practice widely uses the IRP-type grouted anchors in Hungary which are generally installed in sandy or clayey soils. The grouted anchors are also used at the Budapest underground for the construction of subsurface stations.

RESULTS OF FIELD TESTS

In order to investigate the above mentioned problems a testserie was performed on instrumented grauted anchors which allowed the analysis of the behaviour of anchors - under load - installed in granular soil. The lay-out of one anchor including the soil profile with the soil properties, the grouting pressure and the grout consumption is shown on Fig.1. An attempt was made during the tests to install the entire bond length of anchors in the same type of soil. The grouting pressure was generally about 1,0-1,4 MPa but in some cases - mainly during the second grouting - it reached 2,5 MPa too. However, no surface upheavals were observed. At the same time 12 pieces of inclined and vertical test anchors were investigated. Their free and bond lengths were 9 m and 7 m respectively. On the majority of anchors strain gauges were installed at 5-6 levels. At each level three strain gauges were placed. By this way it was possible to observe the value and distribution of anchor force along the whole bond length during the entire loading procedure. All anchors were loaded in cycles and after stressing they

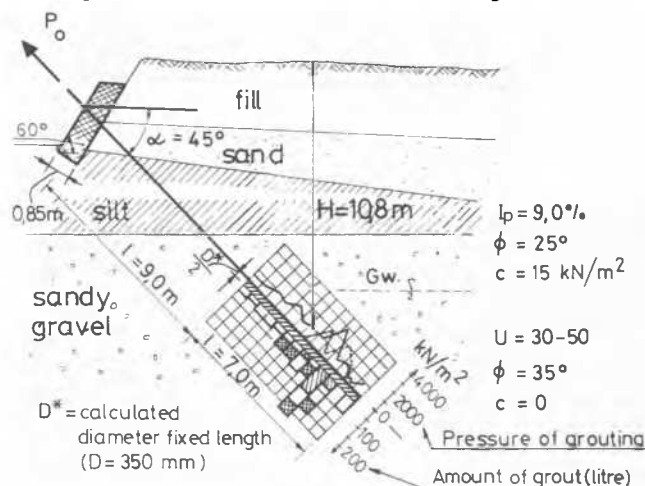


Fig. 1.

were monitored for a year. The alteration of the value of anchor force was continuously recorded by an electric stress-cell put under the anchorhead. Also its distribution was observed along the bond length. One anchor was dug-out after the test and the size of the grouted section as well as the strength of the grouted material was measured. These results facilitated the assumptions of the criteria for the further theoretical analyses.

The upper a/ part of Fig. 2 presents the load-displacement diagram of an anchor inclined to $\alpha = 45^\circ$ while the lower b/ part shows the anchor force calculated from the readings of the strain-gauges at different levels of the bond length. As indicated by the upper part of the figure the anchor was loaded in cycles. The displacement consists of three components:

Δl_0 = elastic elongation of the free anchor length,

Δ = displacement of the retaining wall,

Δl_x = displacement of the bond length.

The strain gauges were installed on the bond length at the distances measured from the anchor end as indicated on the drawing.

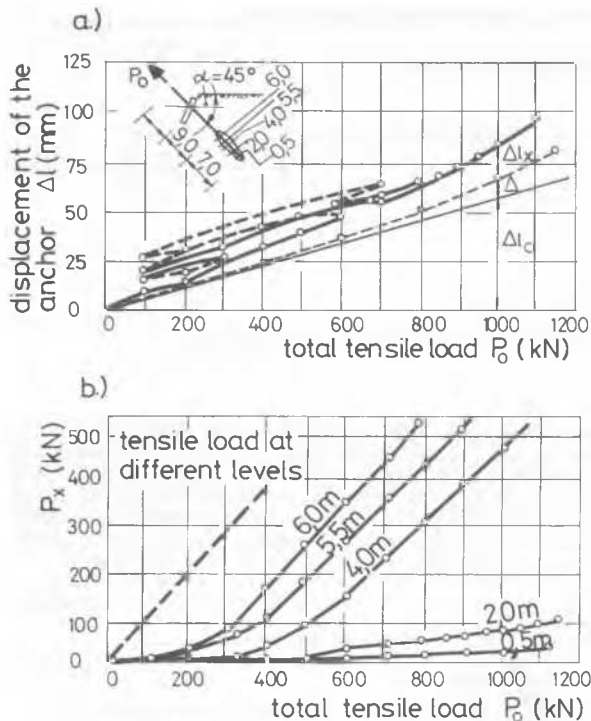


Fig. 2.

The lower part of the figure indicates the amount of the anchor force measured at the different levels of the bond length. It shows that on about a 2 m section of the 7 m long bond length hardly 10 % of the total force - even at a stressing load of $P_0 = 1000$ kN - can be measured, in other words, the anchor end hardly contributes to the load carrying. It clearly demonstrates the reduction rate of anchor force, however the alteration of anchor force along the bond length can be better reviewed after studying the Fig. 3.

Its a/ part presents the alteration of anchor force at different stressing while the b/ part shows the displacements of the bond length at the different anchor forces calculated from the readings of the strain gauges indicated on the c/ part of the figure. Mention should be made of the marking $S_{max} = 4$ mm which indicates the displacement required to mobilize the entire shearing resistance along the bond length. On those portions of the bond length where the displacement reaches or exceeds the S_{max} value as the unit strain ($\epsilon\%$) as the anchor force increases linearly.

The d/ part of the figure indicates the ratio of the unit strain ($\Delta\epsilon$) to the unit bond length (Δx) related to the various anchor forces. At those sections where this ratio reaches the maximum value the shearing resistance is mobilized. Thus it is possible to determine on this detail that portion of the bond length where the shearing resistance is exhausted. This parallel section to the abscisse is in our case $l_1 \approx 2,9$ m.

The determination of that point of the bond length whose displacement is equal or larger than the S_{max} value required to mobilize the shearing resistance provides a reliable basis for the determination not only of the load transfer mechanism of the anchor but also of the safety against its pull-out.

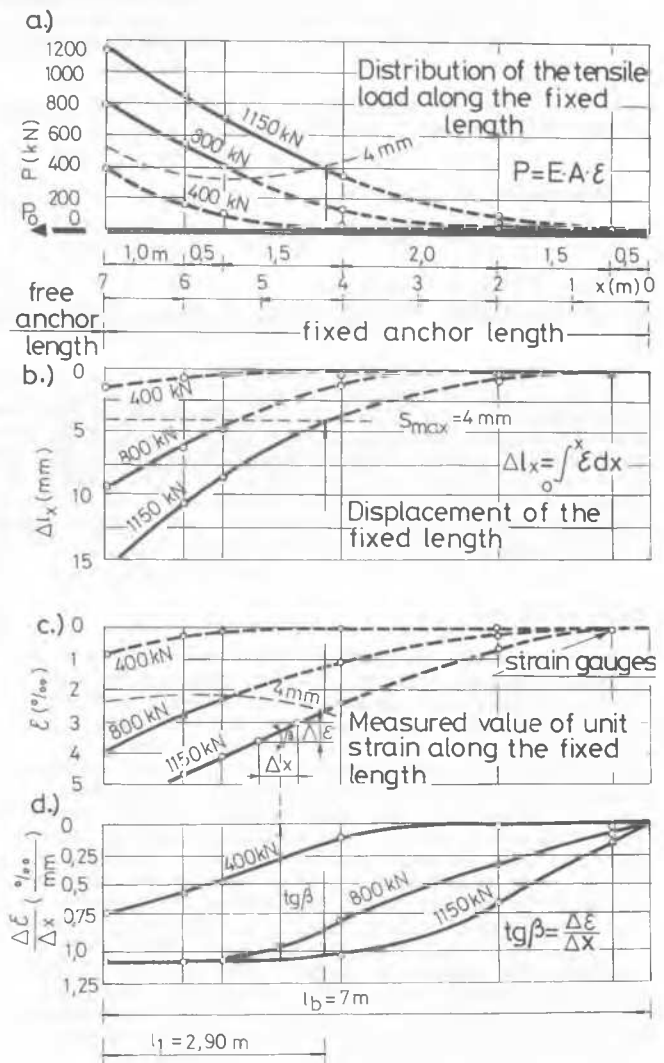


Fig. 3.

The value of τ_{max} and S_{max} - Fig. 3. - depend not only on the type of the soil but on the initial density and the grain-size distribution as well. Moreover these values are significantly affected also by the quality of anchor injection.

The coefficients of the shear-resistance obtained by conventional triaxial or direct shear tests are - in non-cohesive soils - significantly less than it is computable back from the anchor-force. Because of the confined displacements of the grain-size as our analysis indicates, the increase of the angle of the internal friction - for non-cohesive soils - can attain 40 %, depending on the initial density.

Fig. 4. gives the results of the series of experiments which was carried out in sand for the determination of the angle of the internal friction. Triaxial tests were made and the angle of the internal friction was found, in function of the initial compactness between 30 and 34 degrees. Upholding the same compactness we put a model of anchor of diameter $d = 28$ mm into a sample of soil of diameter $D = 100$ mm and of

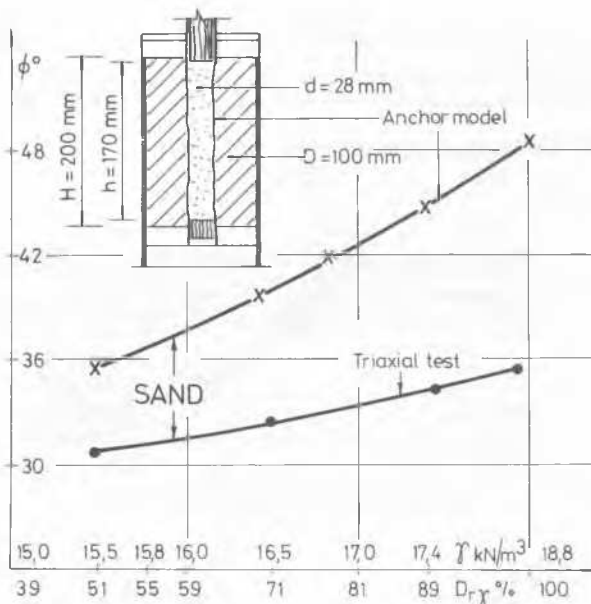


Fig. 4

height $H = 200 \text{ mm}$, and carried out the test upon constant volume. The surface of the model of anchor was coated with plastic resin and aftermath covered by the sand in view. In this manner the shearing takes place between sand and sand. Upholding the constant volume we obtained, in function of the initial compactness significantly greater values of the internal friction: $\phi = 34 - 48$ degrees. The explanation of this change lays in the phenomenon of the dilatation.

The shearing is followed by a kind of dilatation and so the horizontal stress - in sands - increases significantly. In silt this phenomenon is hardly observable, while in clay not at all, that is the methods lead to the same value of angle of the internal friction. We determined the angle of the internal friction referring to the initial diameter of the model.

RESULTS OF ANALYTICAL INVESTIGATION

Presentation of the method.

Applying the experimental results obtained by instrumented anchors we elaborated the following analytical approach.

In the following the treatise will present a method elaborated for the determination of the anticipated load bearing capacity, the distribution of anchors forces along the bond length as well as the elongation and displacement of the grouted anchors.

Let's assume that the soil is elastically plastic and the relationship shown on Fig. 5/a exists between its τ shear stress and the s displacement. Hence the shear stress linearly increases with the displacement to a maximum value. The model assumes as known values as the τ_{\max} shear stress as the s_m displacement required for its mobilization. The model neglects the bearing capacity of an eventual anchor shown on Fig. 5/b.

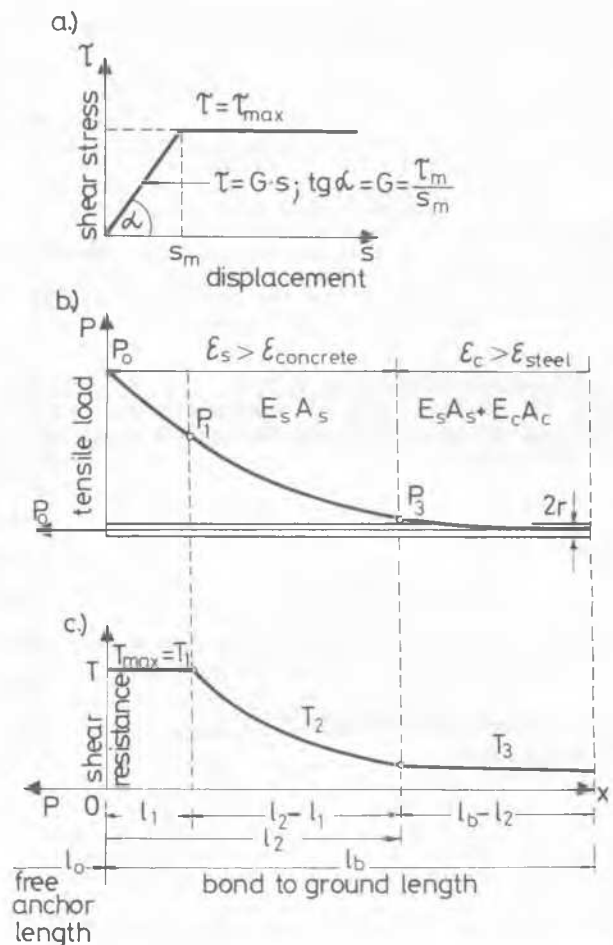


Fig. 5

l_0 = free anchor length

l_1 = that portion of the bond length where the shear stress reaches the maximum value

l_2 = that portion of the bond length where the elongation exceeds the crackfree limit characteristic for the grouted material of a given strength, i.e. on the l_2 length the concrete does not work due to the cracks, while from l_2 to the anchor and /on the $l_b - l_2$ section/ the concrete and steel act together.

The task of the model is to determine the l_1 and l_2 . The solution assumes that l_2 might always be larger than l_1 and at small P forces the case of $l_1 = 0$ might be possible. The $P(l_b) = 0$ condition is further obvious. The relation between P and τ is the following:

$$dP = -2r\pi\tau dx \quad (1)$$

where r is the radius of the bond length of anchor. It results in

$$P(l_1) = P_1 = P_0 - 2r\pi\tau_m \cdot l_1 = P_0 - \tau_m l_1 \quad (2)$$

where $T_m = 2r\pi\tau_m$ and in $(0, l_1)$ $P = P_0 - x T_m$. By the derivation of Equ. (1) for the addition length of the anchor:

$$\frac{d^2P}{dx^2} = -2r\pi \frac{d}{dx} = -2r\pi G \frac{ds}{dx} = 2r\pi G \frac{P(x)}{E A} \quad (3)$$

where the $T = Gs$ relationship was used /s is the displacement in the -X direction/. Thus $G = \frac{T_m}{s_m}$ from the borderline case, while the value /modulus of elasticity times surface/ on the (l_1, l_2) section $E_{steel} \cdot A_{steel}$ as the concrete is tucked here while on the (l_2, l_b) interval $E_s A_s + E_c A_c$. On the (l_2, l_b) section the two border conditions of the differential equations:

$$P(l_b) = 0$$

$$P(l_2) = E_c(E_s A_s + E_c A_c) = P_3 \quad (4)$$

where E_c is the limit of the unitstrain of concrete. At these conditions the solution of the (3) equations:

$$P(x) = P_3 \left(\text{ch}w_1' \frac{x-l_2}{l_b-l_2} - \text{cth}w_2' \cdot \text{sh}w_2' \frac{x-l_2}{l_b-l_2} \right) \quad (5)$$

where

$$w_2' = \frac{T_m(l_b-l_2)}{s_m(E_s A_s + E_c A_c)}$$

On the (l_1, l_2) section the (3) equations must be solved under the following conditions:

$$\begin{aligned} P(l_1) &= P_1 \\ P(l_2) &= P_3 \end{aligned}$$

where P_1 and P_3 are defined in equation (2) and (4) respectively.

On the (l_1, l_2) section the (3) equation must be solved under the following conditions:

$P(l_1) = P_1$, $P(l_2) = P_3$, where P_1 and P_3 are defined in equation (2) and (4) respectively. The solution can be derived exactly as solution (5).

Hence the $P(x)$ function can be constructed for the whole anchor as a function of the unknown l_1 and l_2 . These l_1 and l_2 can be determined from the connecting equations of the shear stresses, while the shear stress is the negative derivative of function $P(x)$. The connecting equations are:

$$\begin{aligned} T_1(l_1) &= T_2(l_1) \\ T_2(l_2) &= T_3(l_2) \end{aligned} \quad (6)$$

where $T_1 = T_m$, the unit shearforce on one meter anchor/ valid for the section $(0, l_1)$ T_2 and T_3 are the negative derivatives of the corresponding $P(x)$ functions of the sections (l_1, l_2) resp. (l_2, l_b) . So (6) gives two equations for l_1 and l_2 . This transcendent equation system was solved numerically considering only the physically understandable cases of the solutions. Hence the elongation of the anchor can be found by the integration of the different $P(x)$ -s on the correspondent sections, and summing them up. Omitting the performance of the integrations the result is:

$$\begin{aligned} \Delta l = & \frac{1}{E_s A_s} \left[P_0 l_0 + P_0 l_1 - \frac{1}{2} T_m l_1^2 \cdot \frac{(\text{ch}w_1' - 1)(P_1 + P_3)}{w_1' \text{sh}w_1'} \right] + \\ & + \frac{1}{w_2'(E_s A_s + E_c A_c)} P_3 [\text{sh}w_2' - (\text{ch}w_2' - 1) \text{cth}w_2'] \end{aligned} \quad (7)$$

The displacement of the anchor tip must be added to it which can be determined from the following relationship:

$$S_0 = \frac{T_3(l_b)}{T_m} \cdot s_m \quad (8)$$

The final elongation and displacement of the anchor is given by the sum of Equ. (7) and (8.)

Application of the Method

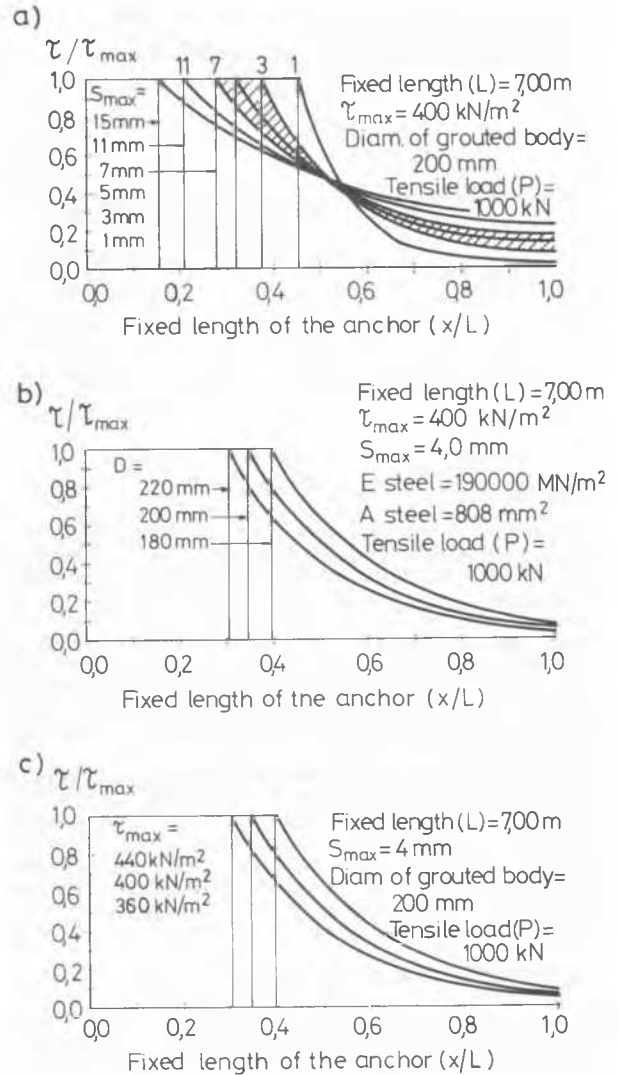


Fig. 6.

Fig. 6. shows the behaviour of the anchor under load respectively the effects of the 3 main parameters on the load holding capacity. The part a/ gives the distribution of the shear stress along the fixed length in function of the different values of S_{max} necessary to mobilize the shear stress. / $S_{max} = 1, 3, 5, 7, 11, 15$ mm/. Although at normal soil conditions the value of S_{max} is between 3 and 7 mm, we extend the computations to a more large interval to facilitate the investigation of the mechanism of the load-transfer. It is perceptible that for $S_{max} = 1$ mm which supposes a more rigid bonding τ_{max} is attained for a longer interval and the shear-force decreases rapidly. On the contrary for $S_{max} = 15$ mm τ_{max} is attained in a shorter interval and the

DISTRIBUTION OF THE LOAD ALONG THE FIXED LENGTH

INC. OF ANCHOR = 45 DEG.
 FIXED LENGTH (L) = 7.00 M
 DIAM. OF GROUTED BODY = 350 MM
 $\tau_{MAX} = 250 \text{ KN/M}^2$
 $S_{MAX} = 4.0 \text{ MM}$
 $E_{STEEL} = 190000 \text{ MN/M}^2$
 $A_{STEEL} = 808 \text{ MM}^2$
 $E_{CONCRETE} = 5000 \text{ MN/M}^2$
 $\sigma_{CONCRETE} = 500 \text{ KN/M}^2$

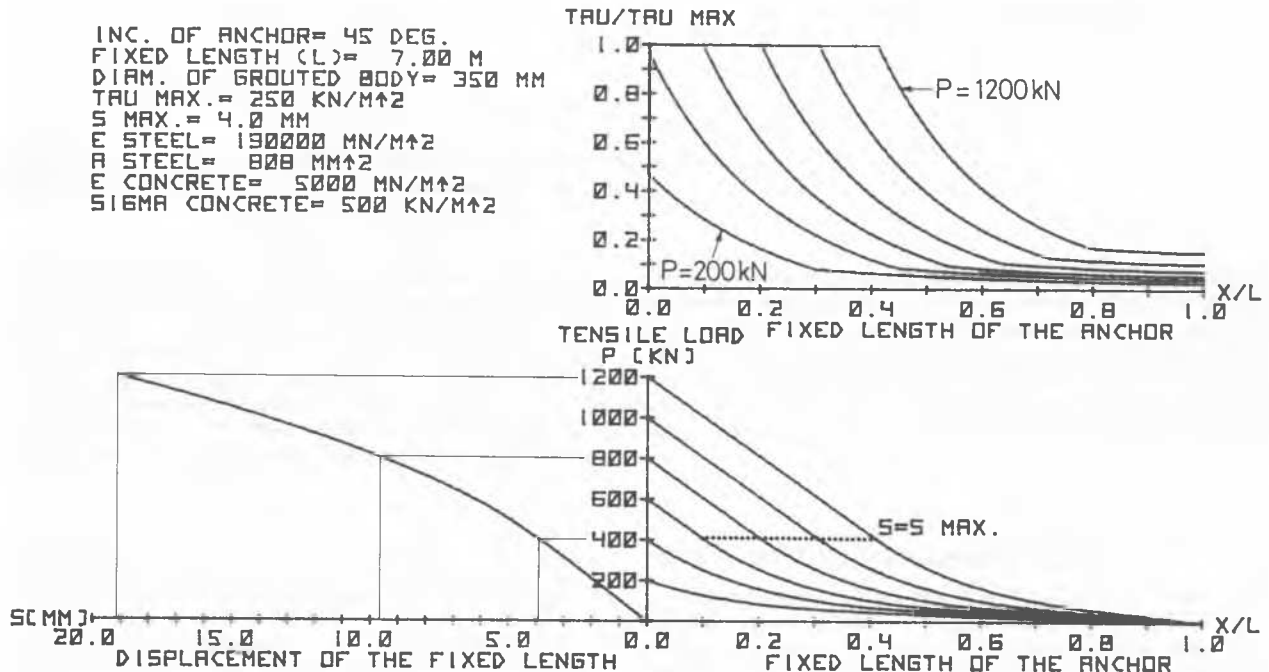


Fig.7.

shear-force decreases more slowly. This phenomenon rises the probability of the development of local defects and increases the danger of the progressive failure. The part b, and c, of Fig. 6 shows the effects of the diameter and of τ_{max} . The increments of the load /about 10 %/ cause predictable changes in the extension of domain of τ_{max} and in the process of the decrease.

Finally some results of the computations are given on Fig. 7. concerning of a concrete practical case.

Fixing the initial parameters Fig. 7. shows

- the change of the shear-stresses along the fixed length of the anchor. The value of S is equal to 1 where the displacement S is greater or equal to 4 mm /right above/
- the change of the tensile force along the fixed length. It is visible that the change of the tensile force is linear where the displacement of the anchor is equal or over the S_{max} /right below/
- The concordance between the two figures is clear.
- The top-displacement in the function of the tensile load /left below/.

CONCLUSIONS

- The determination of the holding capacity of anchors calculated by means of characteristics of soil which is obtained from conventional laboratory tests is not reliable in the case of sands.
- The holding capacity and the load transfer is considerably influenced by the type and the initial compactness of the soil, because on these depends the value of the displacement S_{max} necessary to the total mobilization of the shear-resistance.
- The pressure of the injection has a great influence on the phenomenon because this determines the part of the fixed length on which the shearing resistance is mobilized.

REFERENCES

- Littlejohn, G.S. /1979/ Ground Anchors; State-of-the-art. Symposium on Prestressed Ground Anchors. The Concrete Society of South Africa Prestressed Concrete Division, Johannesburg
- Ostermayer, H. Scheele, F. /1978/ Research on ground anchors in non-cohesive soils. Revue Francaise de Géotechnique No 3. pp 92-97.